Cardiovascular Research (2014) **101**, 326–334
doi:10.1093/cvr/cvt269

Overexpression of *KCNN3* results in sudden cardiac death

Saagar Mahida[1], Robert W. Mills[1], Nathan R. Tucker[1], Bridget Simonson[2], Vincenzo Macri[1], Marc D. Lemoine[3], Saumya Das[2], David J. Milan[1,4], and Patrick T. Ellinor[1,4]*

[1]Cardiovascular Research Center, Massachusetts General Hospital, Charlestown, MA, USA; [2]Cardiovascular Institute, Beth Israel Deaconess Medical Center, Boston, MA, USA; [3]Department of Cardiology and Angiology, Westfälische Wilhelms-University, University Hospital Münster, Münster, Germany; and [4]Cardiac Arrhythmia Service, Massachusetts General Hospital, Boston, MA, USA

Received 18 May 2013; revised 23 November 2013; accepted 25 November 2013; online publish-ahead-of-print 1 December 2013

Time for primary review: 26 days

Background A recent genome-wide association study identified a susceptibility locus for atrial fibrillation at the *KCNN3* gene. Since the *KCNN3* gene encodes for a small conductance calcium-activated potassium channel, we hypothesized that overexpression of the SK3 channel increases susceptibility to cardiac arrhythmias.

Methods and results We characterized the cardiac electrophysiological phenotype of a mouse line with overexpression of the SK3 channel. We generated homozygote ($SK3^{T/T}$) and heterozygote ($SK3^{+/T}$) mice with overexpression of the channel and compared them with wild-type (WT) controls. We observed a high incidence of sudden death among $SK3^{T/T}$ mice (7 of 19 $SK3^{T/T}$ mice). Ambulatory monitoring demonstrated that sudden death was due to heart block and bradyarrhythmias. $SK3^{T/T}$ mice displayed normal body weight, temperature, and cardiac function on echocardiography; however, histological analysis demonstrated that these mice have abnormal atrioventricular node morphology. Optical mapping demonstrated that $SK3^{T/T}$ mice have slower ventricular conduction compared with WT controls ($SK3^{T/T}$ vs. WT; 0.45 ± 0.04 vs. 0.60 ± 0.09 mm/ms, $P = 0.001$). Programmed stimulation in 1-month-old $SK3^{T/T}$ mice demonstrated inducible atrial arrhythmias (50% of $SK3^{T/T}$ vs. 0% of WT mice) and also a shorter atrioventricular nodal refractory period ($SK3^{T/T}$ vs. WT; 43 ± 6 vs. 52 ± 9 ms, $P = 0.02$). Three-month-old $SK3^{T/T}$ mice on the other hand displayed a trend towards a more prolonged atrioventricular nodal refractory period ($SK3^{T/T}$ vs. WT; 61 ± 1 vs. 52 ± 6 ms, $P = 0.06$).

Conclusion Overexpression of the SK3 channel causes an increased risk of sudden death associated with bradyarrhythmias and heart block, possibly due to atrioventricular nodal dysfunction.

Keywords Arrhythmias • Atrial fibrillation • Ion channels • Heart block • Potassium channel

1. Introduction

The SK3 (KCNN3, $K_{Ca}2.3$) channel is one of a family of three small conductance (SK), voltage-independent, calcium-activated potassium channels. The other members of the SK family include SK1 (KCNN1, $K_{Ca}2.1$) and SK2 (KCNN2, $K_{Ca}2.2$). SK channels are gated directly by submicromolar concentrations of intracellular calcium.[1] SK channels, therefore, provide a link between intracellular calcium transients and membrane potassium conductance.[2,3]

SK channels are expressed in excitable tissues such as cardiomyocytes[4,5] and neurons.[6] During neuronal action potentials, activation of SK channels contributes to classical afterhyperpolarization which plays a critical role in the regulation of neuronal firing rate and pattern.[7] The role of SK channels in cardiac electrophysiology is less clearly defined. Previous studies have demonstrated that, in a murine model, knockout of the SK2 channel results in prolongation of the action potential and alterations in the spontaneous firing rate of pacemaker cells.[8,9] The SK3 channel has been demonstrated to form heteromultimeric complexes with the SK2 channel *in vitro*, and blockade of the SK2/3 complex has also been shown to prolong the action potential duration (APD) in isolated cardiomyocytes.[10]

A number of studies have implicated SK channels in the pathogenesis of atrial fibrillation (AF). A recent genome-wide association study identified a susceptibility locus for AF at the *KCNN3* gene.[11] In isolated rabbit atria, burst pacing in the pulmonary veins, which play an important role in the genesis of AF, causes an up-regulation of the KCNN current ($I_{K,Ca}$) with consequent shortening of the action potential.[12] Pharmacological inhibition of SK channels has been reported to suppress AF, an effect

* Corresponding author. Cardiovascular Research Center and Cardiac Arrhythmia Service, 149 13th Street Charlestown, MA 02129, USA. Tel: +1 617 724 8729; fax: +1 617 726 5806, Email: pellinor@partners.org

that is likely to be mediated by prolongation of the atrial effective refractory period (AERP).[13,14] However, the interaction between SK channels and susceptibility to arrhythmias remains unclear: notably, knockout of SK2, which is predicted to attenuate the $I_{K,Ca}$ current, also increases susceptibility to AF.[8] Furthermore, in a canine model, pharmacological blockade of the $I_{K,Ca}$ current increases risk of atrial arrhythmias.[15]

SK channels have also recently emerged as potentially important contributors of ventricular arrhythmias. In a rabbit heart failure model, the $I_{K,Ca}$ current is heterogeneously up-regulated due to increased sensitivity of SK channels to intracellular calcium and pharmacological blockade of $I_{K,Ca}$ eliminates spontaneous ventricular arrhythmias.[16] Similarly, in a rat acute myocardial infarction model, blockade of the $I_{K,Ca}$ current has been reported to prolong the APD and to suppress ventricular arrhythmias.[17]

Based on these observations, we hypothesized that overexpression of the SK3 channel increases susceptibility to cardiac arrhythmias.[18] In the present study, we found that SK3 channel overexpression is associated with sudden death and increases susceptibility to a spectrum of arrhythmic syndromes, including heart block and bradyarrhythmias, AF, and slowed ventricular conduction.

2. Methods

2.1 Generation of mice with overexpression of *Kcnn3*

All animal experiments were approved by the Partners Subcommittee on Research Animal Care (SRAC) and were conducted in compliance with the regulations published in the US National Institute of Health *Guide for the Care and Use of Laboratory Animals*. $SK3^{T}$ mice harbour a tetracycline-based genetic switch upstream of the *Kcnn3* gene. At baseline, the mutant allele results in overexpression of *Kcnn3* while upon administration of tetracycline (or doxycycline), *Kcnn3* expression has been reported to be eliminated.[19] Heterozygote ($SK3^{+/T}$) mice were crossed to generate homozygote ($SK3^{T/T}$), heterozygote ($SK3^{+/T}$), and wild-type (WT) siblings.

Mice were weaned and genotyped at 4 weeks of age by PCR of tail snip DNA. Mice were maintained in a standard facility with controlled temperature and humidity with 12-h light and dark cycles. Food and water were available *ad libitum*. To suppress *Kcnn3* expression, $SK3^{T/T}$ mice were treated with doxycycline (2 mg/mL in drinking water).

Initially, data were obtained from 3-month-old $SK3^{T/T}$, $SK3^{+/T}$, and WT mice. However, a high incidence of sudden death in $SK3^{T/T}$ mice between 20 and 40 days of age prompted evaluation with optical mapping and programmed electrical stimulation in 1-month-old mice to avoid a survival bias.

2.2 Anaesthesia

Mice were anaesthetized to minimize discomfort and stress during *in vivo* electrophysiology studies, implantation of telemetry devices, tail snipping, and prior to euthanasia. Anaesthesia was induced by administering 5% isoflurane (VetOne, USA) driven by an oxygen source into an induction chamber. Anaesthesia was subsequently maintained with 1–2% isoflurane in 95% O_2 delivered via a modified Bain circuit mask's inner tube. Mice were tested for adequate depth of anaesthesia by toe-pinch reflex. Proper anaesthesia was deemed to have been attained when pinching of the paw consistently failed to elicit a reflex. Euthanasia was performed by intraperitoneal administration of sodium pentobarbital 200 mg/kg (Hospira, Lakeford, IL, USA). Once animals were injected, sufficient time was allowed for them to develop respiratory arrest.

2.3 Echocardiography

A GE Vivid 5 with a 15L8 15 MHz linear array transducer at a frame rate of 100 frames/s was used to perform echocardiography. The echocardiograms were performed in the absence of anaesthesia. Mice were trained by repeatedly simulating the procedure. Two-dimensional views were acquired in the short-axis and parasternal long-axis view. M-mode recordings were acquired in the short-axis view at the level of the papillary muscles.

Left ventricular chamber dimensions (left ventricular internal dimension diastole, left ventricular internal dimension systole, and wall thickness) were measured from the M-mode recordings. Left ventricular fractional shortening (FS) and ejection fraction (EF) were calculated as follows:

$$\mathrm{FS}\,(\%) = \left(\frac{\mathrm{LV\,internal\,dimension\,diastole} - \mathrm{LV\,internal\,dimension\,systole}}{\mathrm{LV\,internal\,dimension\,diastole}}\right) \times 100$$

$$\mathrm{EF}\,(\%) = \left(\frac{\mathrm{LV\,end\text{-}diastolic\,volume} - \mathrm{LV\,end\text{-}systolic\,volume}}{\mathrm{LV\,end\text{-}diastolic\,volume}}\right) \times 100$$

2.4 Histology and immunohistochemistry

Heart sections from 3-month-old $SK3^{T/T}$ and WT mice were stained for fibrosis with Masson's trichrome stain (Sigma-Aldrich, St. Louis, USA) using standard protocols. Connexin-43 localization was analysed by staining heart slices with a connexin-43 primary antibody and an horseradish peroxidase-linked secondary antibody (Abcam, MA, USA). Slides were imaged using a fluorescence microscope (Leica DMIRB).

For analysis of atrioventricular nodal morphology, extracted hearts were snap frozen in OCT and sectioned at 10 μM. Sections were stained with an anti-HCN4 primary antibody (Alamone Labs, Jerusalem, Israel) and a goat anti-rabbit secondary antibody (Molecular Probes, OR, USA). The sections were mounted with Hard Set mounting medium with 4′,6-diamidino-2-phenylindole (Vectashield, Burlingame, CA, USA) and imaged on a Zeiss LSM 510 Meta confocal microscope.

2.5 Optical mapping

Isolation and perfusion of the heart was performed as previously described.[20,21] Briefly, the mouse was anaesthetized using isoflurane, the heart excised, and perfused via an aortic cannula. The cannulated heart was perfused with a modified Tyrode solution (128.2 mM NaCl, 4.7 mM KCl, 1.19 mM NaH_2PO_4, 1.05 mM $MgCl_2$, 1.3 mM $CaCl_2$, 20.0 mM $NaHCO_3$, 11.1 mM glucose; pH 7.35 ± 0.05)[21] using a Langendorff perfusion setup. Blebbistatin (10 μM, Tocris Bioscience, MO, USA) was used to arrest cardiac motion. The heart was stained for 30 min with a voltage sensitive dye (di-4-ANEPPs, 2 mmol/L in Dimethyl sulfoxide).

Custom-made epicardial platinum electrodes and a Medtronic stimulator were used to pace the heart. Pacing was performed at a 150 ms cycle length at twice the capture threshold (1 ms square wave stimuli). A halogen light source (X-Cite 150 W, filtered at 520 ± 45 nm) was used to excite fluorescence. Emissions >610 nm were collected and focused onto an 80 × 80 CCD camera (RedShirt Imaging SMQ Camera and Macroscope IIA) using a 50 mm ×2.7 lens (numerical aperture 0.4). Data sampling was performed at 2000 frames per s with a filter setting of 1 kHz. A specifically designed Matlab program was used to perform data analysis in order to generate conduction velocities and APD at 80% repolarization.

2.6 Electrophysiology studies

Electrophysiology studies were performed in 1-month-old mice as previously described.[8,22] The anaesthetized mouse was intubated and ventilated via a tracheostomy. A jugular cutdown was performed to gain access to the right internal jugular vein. An octapolar catheter (Millar Instruments, TX, USA) was positioned in the right atrium and ventricle via the jugular vein. Programmed electrical stimulation was performed using a standard protocol with 100 ms drive trains and single extrastimuli to measure function of the atrioventricular node and the conduction properties of atrial and ventricular tissue. The Wenckebach cycle length was measured by progressively faster atrial pacing rates. Sinus node function was determined by measuring the sinus node recovery time (SNRT) following 20 s of pacing at three cycle

lengths (120, 100, and 80 ms). Burst pacing was performed with eight 50 ms bursts and four 30 ms burst episodes up to a total burst pacing duration of 1 min. Programmed electrical stimulation for induction of arrhythmias was performed with single, double, and triple extrastimuli up to a minimum coupling interval of 10 ms as previously described.[8]

2.7 Implantable loop recording

Continuous ambulatory monitoring was performed in ~1-month-old $SK3^{T/T}$ mice by implanting an ETA-F10 transmitter (Data Sciences International, MN, USA). The procedure was performed as previously described.[23] Under local anaesthesia with 2% lidocaine (MP Biomedicals, OH, USA) and general anaesthesia with isoflurane (Vet One, USA), the transmitter was implanted in the abdomen and tunnelled leads were placed in the modified lead II position. Telemetry data was recorded continuously via a receiver placed under the mouse cage. The data were imported for analysis using the ChartPro software (ADInstruments, CO, USA).

2.8 Quantitative PCR

Cardiac tissue was homogenized and total RNA isolated using Trizol reagent (Invitrogen, CA, USA) according to the manufacturer's instructions. The Superscript III kit (Invitrogen) was used to reverse transcribe the RNA to cDNA. Primer pairs for *Kcnn3* and *β actin* were designed to span intronic boundaries. Real-time PCR was performed using the GeneAmp PCR System 9600 thermocycler (Perkin–Elmer, CT, USA). Analysis was performed using the delta–delta C_T method normalized to *β actin*. *Kcnn3* expression levels in $SK3^{T/T}$ and $SK3^{+/T}$ mice relative to WT siblings were expressed as a fold difference.

2.9 Statistical analysis

Data analysis was performed using the Student's *t*-test. A *P*-value of <0.05 was considered as statistically significant. Data were presented as mean values ± standard deviation.

3. Results

3.1 Generation of $SK3^{T/T}$ and $SK3^{+/T}$ mice

We characterized a mouse line with a tetracycline-based genetic switch upstream of the *Kcnn3* gene. At baseline, $SK3^{T/T}$ (homozygote) mice displayed an up-regulation of *Kcnn3* expression in all four cardiac chambers compared with WT controls. The most marked overexpression was observed in the ventricles (*Figure 1A*) . $SK3^{+/T}$ (heterozygote) mice also displayed up-regulation of *Kcnn3* expression; however, the difference in expression levels was more subtle (*Figure 1B*). In $SK3^{T/T}$ mice treated with doxycycline (designated $SK3^{T/T}$ + DOX), *Kcnn3* expression was suppressed and was comparable with that observed in WT controls (see Supplementary material online, *Figure S2*). Due to the limitations of the anti-KCNN3 antibody, we were unable to determine relative SK3 protein expression levels in $SK3^{T}$ mice.

$SK3^{T/T}$ mice demonstrated normal growth and achieved similar body weights to WT siblings (see Supplementary material online, *Figure S6*). Histological analysis did not demonstrate any structural cardiac abnormalities in $SK3^{T/T}$ mice. Specifically, haematoxylin-eosin staining did not reveal abnormal hypertrophy, dilatation, or myofibrillar disarray. Masson's trichrome staining revealed an absence of myocardial fibrosis (see Supplementary material online, *Figure S1*). Echocardiographic analysis also revealed structurally normal hearts in $SK3^{T/T}$ and $SK3^{+/T}$ mice. There were no significant differences in left ventricular dimensions and systolic function in 3-month-old $SK3^{T/T}$ and $SK3^{+/T}$ mice compared with age-matched WT mice (*Table 1*).

3.2 Sudden death in $SK3^{T/T}$ mice

We observed a high incidence of premature sudden death in $SK3^{T/T}$ mice. As demonstrated in the Kaplan–Meier survival curves in *Figure 2*, by the age of 3 months, 7 of 19 $SK3^{T/T}$ males had died suddenly, while there was no mortality observed among $SK3^{+/T}$ ($n = 42$) and WT mice ($n = 55$). The highest mortality was observed between the ages of 20 and 40 days. We did not observe any abnormal behaviour or appearance in the days preceding death. Interestingly, we found that administration of doxycycline silenced SK3 overexpression and resulted in a rescue of the sudden death phenotype (*Figure 2* and see Supplementary material online, *Figure S2*). Of 25 $SK3^{T/T}$ males treated with doxycycline ($SK3^{T/T}$ + DOX), none died suddenly.

3.3 Ambulatory monitoring in $SK3^{T/T}$ mice

To determine the mechanism of sudden death in $SK3^{T/T}$ mice, ambulatory cardiac monitoring was performed in 1-month-old $SK3^{T/T}$ mice ($n = 6$) and WT mice ($n = 2$). Of six $SK3^{T/T}$ mice that underwent ambulatory monitoring, four died suddenly. In one of the mice, however, death occurred within 10 days of implantation of the telemetry device. Based on the fact that this mouse may have died due to a complication related to device implantation, it was excluded from further analysis.

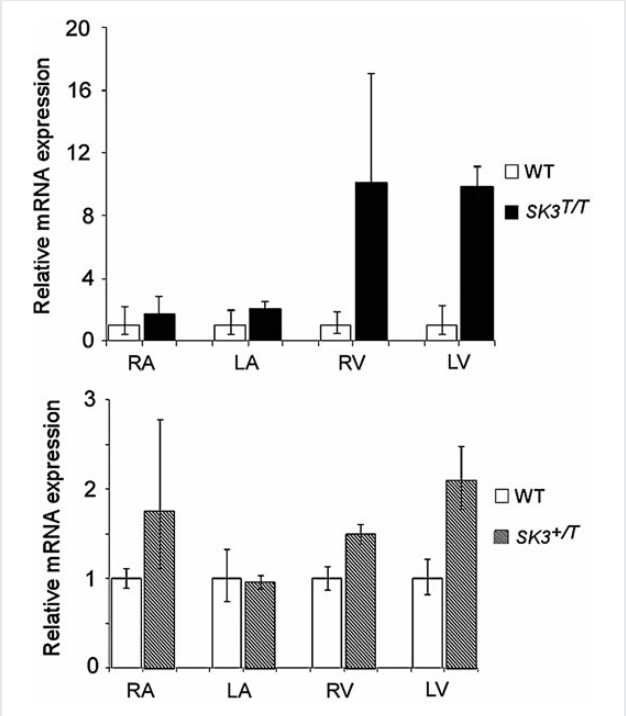

Figure 1 Comparison of *KCNN3* expression in $SK3^{T/T}$, $SK3^{+/T}$, and WT mice by reverse transcription-polymerase chain reaction. *KCNN3* mRNA levels were quantified in all four cardiac chambers and normalized to β-actin expression. Results are expressed as fold change relative to expression levels in WT controls. Error bars represent the standard error of mean. (*A*) $SK3^{T/T}$ mice display up-regulation of *KCNN3* expression in all four cardiac chambers when compared with WT mice. The most marked overexpression was seen in the ventricles (*$P < 0.01$). (*B*) $SK3^{+/T}$ mice display up-regulation of *KCNN3* expression; however, the up-regulation was less pronounced. RA, right atrium; LA, left atrium; RV, right ventricle; LV, left ventricle.

Table 1 Echocardiographic measurements in 3-month-old mice

	LVEDD (mm)	LVESD (mm)	IVSD (mm)	PWD (mm)	FS (%)	EF (%)
WT ($n = 15$)	3.0 ± 0.2	1.5 ± 0.2	0.8 ± 0.1	0.8 ± 0.01	48 ± 8	85 ± 6
$SK3^{+/T}$ ($n = 13$)	3.2 ± 0.2	1.6 ± 0.1	0.7 ± 0.01	0.8 ± 0.01	50 ± 1	87 ± 1.1
$SK3^{T/T}$ ($n = 5$)	3.0 ± 0.4	1.5 ± 0.1	0.8 ± 0.02	0.8 ± 0.05	53 ± 4	89 ± 3

LVEDD, left ventricular end-diastolic dimension in diastole; LVESD, left ventricular end-systolic dimension; IVSD, interventricular septal dimension in diastole; PWD, posterior wall dimension in diastole; FS, fractional shortening; EF, ejection fraction.

The cardiac rhythm recorded at the time of death in two of the three remaining mice that died suddenly was heart block followed by severe bradycardia. We were unable to record the rhythm in the third $SK3^{T/T}$ mouse due to depletion of the battery in the monitoring device. The first mouse, $SK3^{T/T}$ (1), had bradycardia with sinus arrest and advanced atrioventricular conduction block (*Figure 3B*). The second mouse, $SK3^{T/T}$ (2), had bradycardia with a pronounced first-degree atrioventricular block (PR interval 52 ms, normal range in age-matched C57BL/6J mice 29.4 ± 4.5)[24] and evidence of interventricular conduction delay (*Figure 3C*). Neither of the WT mice died during ambulatory monitoring.

During the period of ambulatory monitoring, $SK3^{T/T}$ mice had a lower mean heart rate compared with WT mice. $SK3^{T/T}$ mice displayed frequent episodes of atrioventricular dissociation, both at rest and during periods of activity (see Supplementary material online, *Figure S3*). $SK3^{T/T}$ mice also displayed more pronounced variability of the heart rate and the PR interval. The results are summarized in *Table 2*, *Figure 4*, and Supplementary material online, *Figure S4*.

The body temperature of the $SK3^{T/T}$ and WT mice was also recorded during ambulatory monitoring. Five of the six $SK3^{T/T}$ mice and both WT mice demonstrated normal temperature recordings throughout the monitoring period. One $SK3^{T/T}$ mouse that died within 10 days of device implantation displayed significant hypothermia (average temperature 31.7°C) throughout the recording. Since it was unclear if the hypothermia was due to a calibration issue with the monitor, an adverse reaction to anaesthesia, or a failure to recover fully from the surgery, to be conservative we excluded this mouse from further analysis. The results from ambulatory temperature monitoring are summarized in Supplementary material online, *Figure S7*.

3.4 Atrioventricular node histology in SK3$^{T/T}$ mice

To further investigate the potential mechanisms underlying atrioventricular block in $SK3^{T/T}$ mice, we performed histological analysis of the atrioventricular node in 5-month-old mice. $SK3^{T/T}$ and WT mice both exhibited increased HCN4 immunoreactivity, which is characteristic of the atrioventricular node (see Supplementary material online, *Figure S8*). However, when compared with control, the $SK3^{T/T}$ mouse displayed an overtly enlarged and disorganized nodal structure combined with an increased observance of pyknotic nuclei, a phenotype which could explain the lack of conduction resulting in the atrioventricular block observed in *Figure 3*.

3.5 Ventricular conduction velocities and action potential duration in SK3$^{T/T}$ mice

Optical mapping of isolated, Langendorff-perfused hearts from $SK3^{T/T}$, $SK3^{+/T}$, and WT mice was performed at 1 month of age. We selected this time point due to a high incidence of sudden death among $SK3^{T/T}$ mice between the ages of 20 and 40 days. $SK3^{T/T}$ mice displayed a significantly slower ventricular conduction velocity when compared with WT mice (*Figure 5A*). We also observed a trend towards slower ventricular conduction in $SK3^{+/T}$ mice. A representative example of the ventricular activation pattern during pacing at 150 ms from the left ventricular apex is demonstrated in *Figure 5B*. We did not observe significant differences in the APD_{80} between $SK3^{T/T}$, $SK3^{+/T}$, and WT mice. However, we did observe a marked increase in the dispersion in the APD_{80} in $SK3^{T/T}$ mice (*Figure 5C* and *D*).

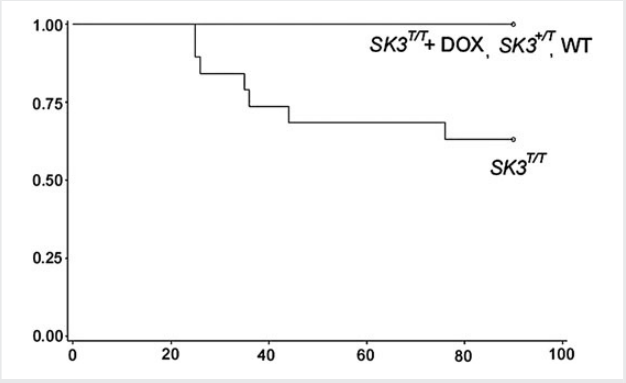

Figure 2 Sudden death in $SK3^{T/T}$ mice. Kaplan–Meier survival plot of male WT ($n = 42$), $SK3^{+/T}$ ($n = 55$), $SK3^{T/T}$ + DOX ($n = 25$), and $SK3^{T/T}$ ($n = 19$) mice at 90 days. Cumulative survival rate is plotted against age (days). $SK3^{T/T}$ mice demonstrated a marked increase in the incidence of sudden death between the ages of 20 and 40 days.

3.6 Programmed stimulation in SK3$^{T/T}$ and SK3$^{+/T}$ mice

Programmed electrical stimulation in $SK3^{T/T}$ and $SK3^{+/T}$ mice was performed at 1 and 3 months of age. At 1 month, both $SK3^{T/T}$ and $SK3^{+/T}$ mice displayed inducible AF/atrial arrhythmias. Three of the six $SK3^{T/T}$ mice and one of the five $SK3^{+/T}$ mice had inducible atrial arrhythmias. Atrial arrhythmias were defined as arrhythmias that lasted for more than five consecutive beats. None of the eight age-matched WT mice had atrial arrhythmias. $SK3^{T/T}$ mice also displayed spontaneous atrial premature beats during ambulatory monitoring. The results are summarized in *Figure 6*. Of note, at a 3-month time point, we did not observe atrial arrhythmias in $SK3^{T/T}$, $SK3^{+/T}$, or WT mice.

One-month-old $SK3^{T/T}$ mice demonstrated an abbreviated atrioventricular nodal effective refractory period (AVNERP) compared with WT mice during programmed stimulation. Furthermore, both $SK3^{T/T}$

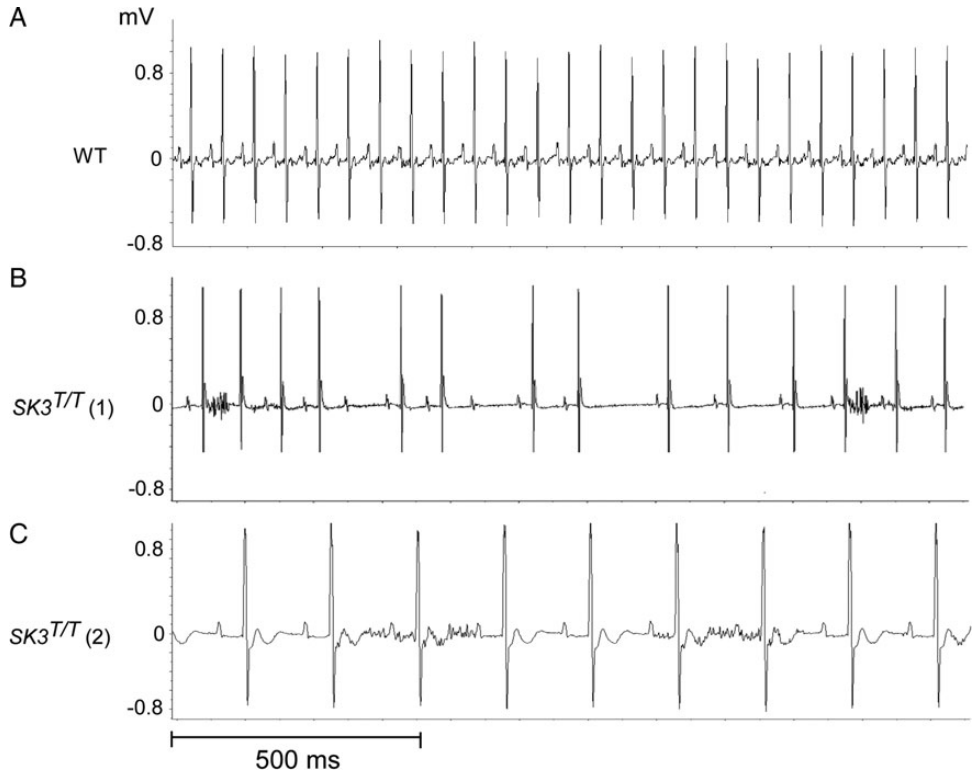

Figure 3 Representative telemetry recordings from $SK3^{T/T}$ mice at the time of sudden death. (*A*) Normal sinus rhythm in a WT mouse demonstrating normal PR interval and heart rate. (*B*) Severe bradycardia with sinus arrest and atrioventricular block in $SK3^{T/T}$ mouse (number 1). (*C*) Severe sinus bradycardia with first-degree atrioventricular block (PR interval 52 ms, normal range in C57BL/6J mice 29.4 $\pm$ 4.5) in $SK3^{T/T}$ mouse (number 2). The voltage of the QRS complexes (mV) is depicted on the *y*-axis and time (s) is depicted on the *x*-axis mV, millivolts.

Table 2 Baseline conduction intervals in 3-month-old mice

Mouse	PR median	PR IQR	RR median	RR IQR
$SK3^{T/T}$ (1)	37.5	0.9	103	20.7
$SK3^{T/T}$ (2)	N.R.	N.R.	111	27.7
$SK3^{T/T}$ (3)	36	3.7	140	37
$SK3^{T/T}$ (4)	35	2.4	141	55
$SK3^{T/T}$ (5)	40.8	1.5	129	30
WT (1)	34.4	1.5	99	13.9
WT (2)	N.R.	N.R.	112	17

N.R., no recording; IQR, inter-quartile range.

and $SK3^{+/T}$ mice displayed abbreviated Wenckebach cycle lengths. Among 3-month-old $SK3^{T/T}$ mice on the other hand, we observed a trend towards a prolonged AVNERP. These mice also have a trend towards a more prolonged SNRT. The results are summarized in *Tables 3* and *4*.

3.7 Connexin-43 expression in $SK3^{T/T}$ mice

Connexin-43 is a major determinant of the ventricular conduction velocity.[25] To exclude altered connexin-43 expression as the cause of reduced conduction velocity in $SK3^{T/T}$ mice, we performed immunohistochemical staining. Hearts from 3-month-old $SK3^{T/T}$ mice were compared with WT mice. We did not observe significant changes in connexin-43 expression or differences in connexin-43 localization between the two groups. Consistent with previous studies, connexin-43 was demonstrated to localize to the borders between myocytes[25] (see Supplementary material online, *Figure S5*).

4. Discussion

In the present study, we examined the role of the SK3 channel in cardiac electrophysiology by characterizing a mouse line that overexpressed the SK3 channel. We found that homozygote mice with overexpression of *Kcnn3* ($SK3^{T/T}$) had overtly normal cardiac function and yet had a high incidence of sudden death. While acute extracardiac causes, including respiratory failure and neurological events, cannot be fully excluded, we believe that primary heart block and bradycardia are the most likely explanation. Interestingly, the atrioventricular node in $SK3^{T/T}$ mice was enlarged and had an abnormal structure. Furthermore, $SK3^{T/T}$ mice had slowed ventricular conduction and increased ventricular repolarization heterogeneity. Both $SK3^{T/T}$ and heterozygote $SK3^{+/T}$ mice had an increased susceptibility to AF and atrial arrhythmias. In summary, our results indicate that the SK3 channel has a role in atrial, atrioventricular nodal, and ventricular conduction (see Supplementary material online, *Figure S9*).

Previous studies have demonstrated that overexpression of the SK2 channel, which can exist in a heteromultimeric complex with the SK3 channel, results in sinoatrial and atrioventricular nodal dysfunction.

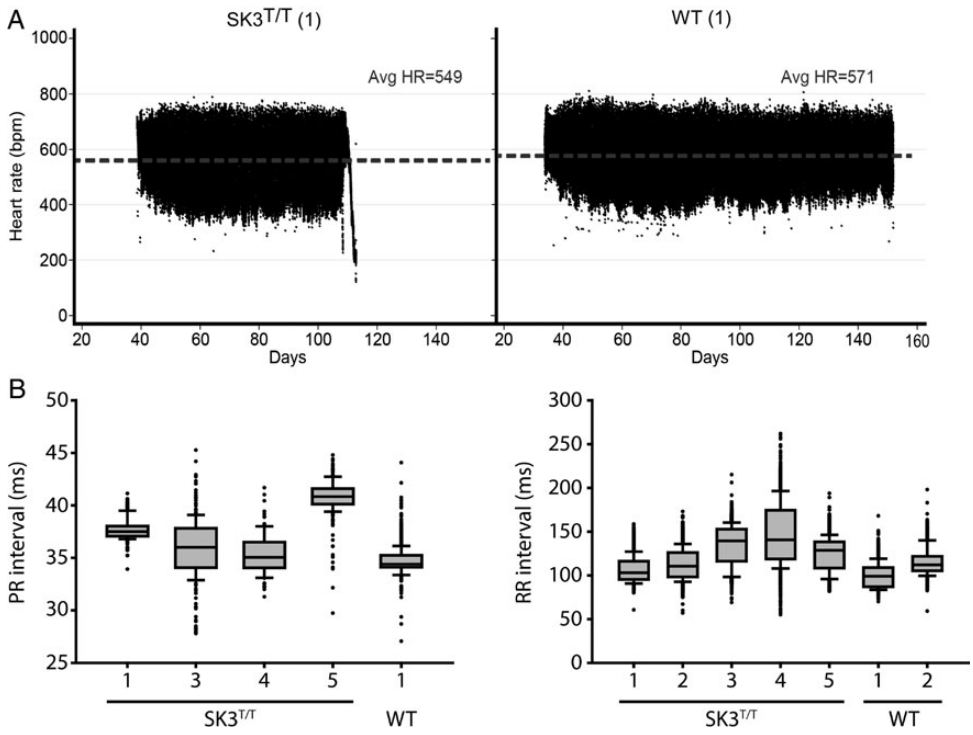

Figure 4 Heart rate and PR interval in conscious WT and *SK3*$^{T/T}$ mice recorded by telemetry. (*A*) Representative scatter plots of continuous heart rate monitoring in *SK3*$^{T/T}$ and WT mice. *SK3*$^{T/T}$ mice display a lower average heart rate and increased heart rate variability. (*B*) *SK3*$^{T/T}$ display increased variability in the PR and RR intervals recorded at 3 months of age.

Zhang *et al.*[9] reported that overexpression of the SK2 channel results in a shortening of the action potential duration in atrioventricular nodal myocytes, while knockout of the channel has the opposite effect. Furthermore, Li *et al.*[8] demonstrated that SK2 null mice have a prolonged sinus node recovery period and Wenckebach cycle length. Consistent with these findings, we observed a shortening of the Wenckebach cycle length and AVNERP in 1-month-old *SK3*$^{T/T}$ and *SK3*$^{+/T}$ mice compared with control mice. In contrast, 3-month-old *SK3*$^{T/T}$ mice had a trend towards prolonged atrioventricular node and sinus node recovery periods, findings consistent with the atrioventricular conduction block we observed on ambulatory monitoring.

While the SK1 and SK2 channel subtypes are predominantly expressed in the atrium, SK3 is expressed in the atrium and the ventricle.[5] This expression profile suggests that the SK3 channel plays a potentially important role in ventricular repolarization. Chua *et al.* previously reported that, in a rabbit heart failure model, up-regulation of the $I_{K,Ca}$ current increases repolarization heterogeneity and susceptibility to recurrent ventricular arrhythmia.[26] Similar results have also been reported in rat models with acute myocardial infarction.[17] In a more recent study, Chang *et al.*[27] found that blockade of the $I_{K,Ca}$ current in a rabbit heart failure model induces triggered activity and torsades des Pointes. These findings imply that $I_{K,Ca}$ is an important contributor to maintaining repolarization reserve in failing hearts. The identification of slowed ventricular conduction and augmented repolarization heterogeneity in *SK3*$^{T/T}$ mice further expands on the role of SK channels.

Our findings are largely consistent with those of *Zhang et al.* in the accompanying manuscript. Similarly, they also observed a high incidence of sudden death among *SK3*$^{T/T}$ mice and no reported mortality among *SK3*$^{+/T}$ and WT mice. In their study, which focused on the role of the SK3 channel in atrial myocytes, they found that overexpression of the channel results in an abbreviated action potential while suppression of channel expression has the opposite effect. In contrast to the findings from Zhang *et al.* discussed above, we did not demonstrate alterations in the AERP in *SK3*$^{T/T}$ mice. Since they observed significantly higher expression of the SK3 channel in *SK3*$^{T/T}$ mouse atria compared with those observed in our study, it is possible that the more pronounced up-regulation of SK3 channel expression may account for the more abbreviated AERP observed in their study.

The results of the present study indicate that overexpression of the SK3 channel creates a pro-fibrillatory substrate in the atrium. Our results are further supported by the elegant recent study by Qi *et al.*[28] They observed that, in a canine model subjected to atrial tachypacing, up-regulation of the $I_{K,Ca}$ current is associated with an increased susceptibility to AF and appears to promote the maintenance of the arrhythmia. Furthermore, they demonstrated that the $I_{K,Ca}$ current is larger in the pulmonary veins when compared with the left atrium. Atrial tachypacing was associated with an increased open probability of SK channels. Quantification of channel expression demonstrated higher SK2 channel expression in the pulmonary veins relative to the left atrium and up-regulation of SK1 channel expression in response to atrial tachypacing. Of note, however, SK3 channel expression was not significantly altered, either between the pulmonary veins and left atrium or in response to atrial tachypacing. Ultimately, further research will be necessary to characterize the precise role of the SK3 channel in the pathogenesis of AF.

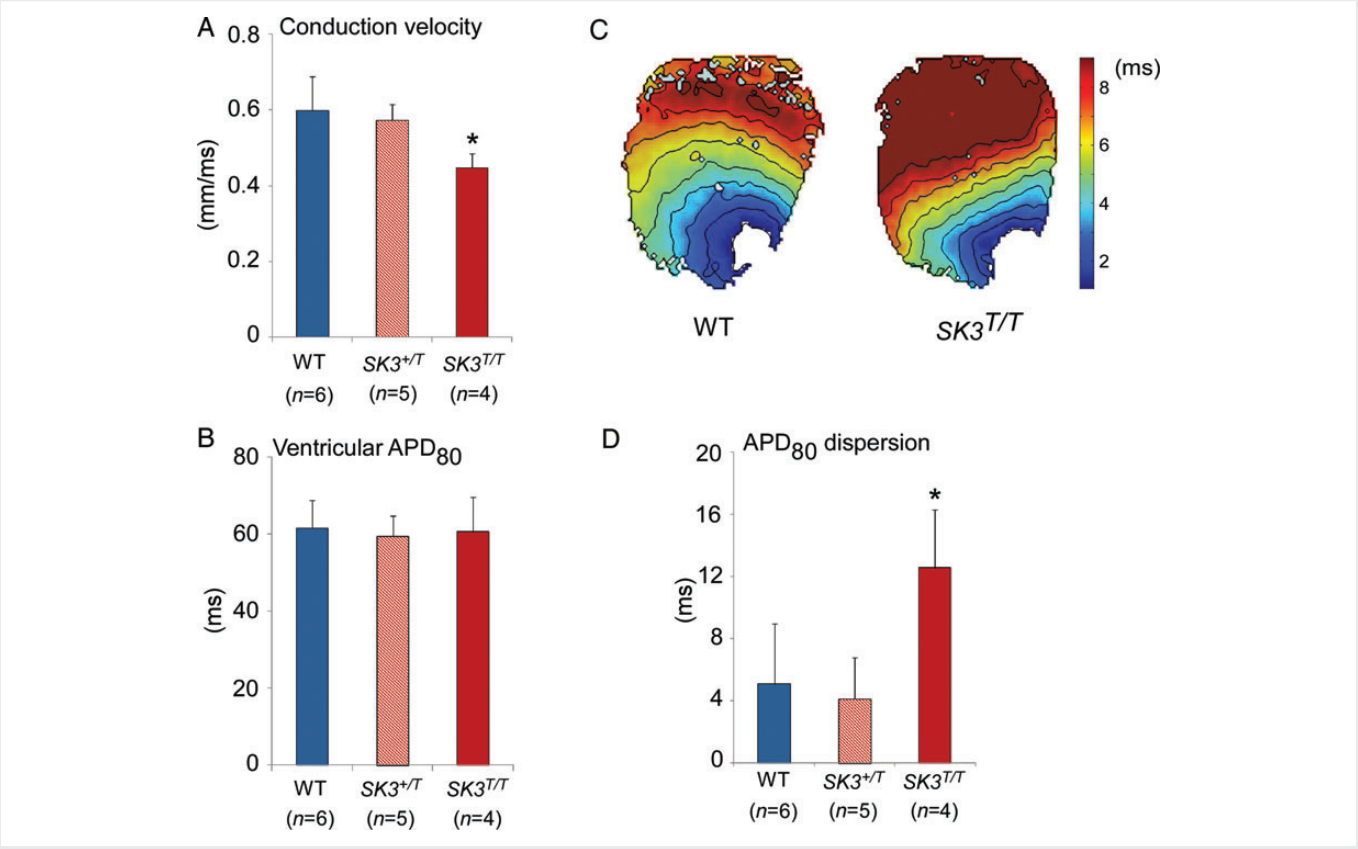

Figure 5 High-resolution optical mapping in isolated $SK3^{T/T}$, $SK3^{+/T}$, and WT mouse hearts. (*A*) Ventricular conduction velocity at a pacing cycle length of 150 ms in 1-month-old $SK3^{T/T}$, $SK3^{+/T}$, and WT mice. Conduction velocity was significantly slower in $SK3^{T/T}$ mice (CV 0.45 $\pm$ 0.04 vs. 0.60 $\pm$ 0.09 mm/ms, $P = 0.001$). (*B*) Representative example of ventricular activation maps on the anterior surface of the heart in a WT and $SK3^{T/T}$ mouse. Hearts were paced from the left ventricular apex at a cycle length of 150 ms, and epicardial activation was recorded as it spread from the apex to the base. (*C*) $SK3^{T/T}$ and $SK3^{+/T}$ mice do not display significant differences in APD_{80} when compared with WT mice. (*D*) $SK3^{T/T}$ display increased dispersion of the APD_{80} when compared with WT mice. $SK3^{+/T}$ mice on the other hand do not display differences in APD_{80} dispersion. APD measurements were made at a pacing cycle length of 150 ms. APD_{80}, action potential duration at 80% repolarization.

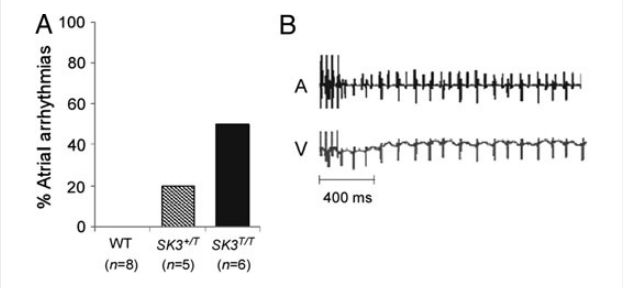

Figure 6 Programmed electrical stimulation in $SK3^{T/T}$, $SK3^{+/T}$, and WT mice. (*A*) Percentage of 1-month-old WT, $SK3^{+/T}$, and $SK3^{T/T}$ mice with inducible AF/atrial arrhythmias on programmed electrical stimulation. (*B*) Representative example of induction of AF after rapid atrial pacing (cycle length 30 ms) in an $SK3^{T/T}$ mouse. The top tracing is an intracardiac electrogram from the atrioventricular junction (A) demonstrating atrial and ventricular activity. The lower tracing is an intracardiac electrogram from the right ventricular apex (V) demonstrating ventricular activity. The intracardiac electrograms demonstrate rapid atrial activity with variable conduction to the ventricle.

5. Limitations

The present study was subject to a number of limitations. Previous studies have demonstrated that mice with variable expression of the SK3 channel have abnormal respiratory responses to hypoxia and seizure activity.[19,29] Furthermore, it has been reported that parasympathetic hyperactivity in mice with seizures and profound hypoxia can result in severe bradycardia.[30,31] Therefore, it is plausible that sudden death is a consequence of neurological or respiratory dysfunction, and that bradycardia and heart block is a secondary phenomenon. While we did not observe seizure activity or abnormal respiratory function in $SK3^{T/T}$ mice in the days preceding death, we also did not witness the episodes of sudden death and are therefore unable to definitively exclude alternative mechanisms of sudden death.

Given that the localization of potassium channels is very dynamic, it is likely that $SK3^{T/T}$ mice have marked alterations in SK3 channel distribution in atrial and ventricular myocytes. However, channel distribution was not characterized in the present study. Furthermore, the I_{KCa} current and action potential were not measured directly in ventricular myocytes.

Table 3 Baseline intracardiac conduction intervals in 1-month-old mice

	SNRT (ms)	AVNERP (ms)	AERP (ms)	AV WB (ms)	VERP (ms)
WT ($n = 8$)	184 ± 32	52 ± 9	30 ± 3	87 ± 6	30 ± 5
$SK3^{+/T}$ ($n = 5$)	150 ± 27	49 ± 2	30 ± 2	**77 ± 5***	31 ± 5
$SK3^{T/T}$ ($n = 6$)	180 ± 46	**43 ± 6***	31 ± 5	**71 ± 4****	31 ± 7

Statistically significant *P* values are in bold.
SNRT, sinus node recovery time; AV WB, atrioventricular Wenckebach cycle length.
*$P < 0.05$.
**$P < 0.01$.

Table 4 Baseline intracardiac conduction intervals in 3-month-old mice

	SNRT (ms)	AVNERP (ms)	AERP (ms)	AV WB (ms)	VERP (ms)
WT ($n = 9$)	98 ± 50	52 ± 6	34 ± 2	90 ± 7	43 ± 9
$SK3^{+/T}$ ($n = 13$)	88 ± 48	50 ± 9	36 ± 4	81 ± 10	38 ± 6
$SK3^{T/T}$ ($n = 3$)	124 ± 52	61 ± 1	34 ± 6	88 ± 2	38 ± 2

Measurements of refractory periods were made using a basic cycle length of 100 ms. Data are expressed as mean ± standard deviation.
SNRT, sinus node recovery time; AVNERP, atrioventricular nodal effective refractory period; AERP, atrial effective refractory period; AV WB, atrioventricular Wenckebach cycle length; VERP, ventricular effective refractory period.

6. Conclusions

We have demonstrated that increased expression of the SK3 channel increases the risk of sudden cardiac death due to bradyarrhythmias. Overexpression of this channel also increases susceptibility to atrial arrhythmias. Our findings suggest that the SK3 channel plays an important role in normal cardiac impulse propagation and arrhythmia susceptibility.

Supplementary material

Supplementary material is available at *Cardiovascular Research* online.

Conflict of interest: none declared.

Funding

This work was supported by the National Institutes of Health (7K08HL089319 to S.D., 5R21DA026982 and 5R01HL109004 to D.J.M., 5T32HL007298-35 to R.M. and N.R.T., 5R21DA027021, 1RO1HL104156, and 1K24HL105780 to P.T.E.); and the American Heart Association (13EIA14220013 to P.T.E.); and the Biotronik and Heart Rhythm Society Postdoctoral fellowship award to (V.M.).

References

1. Adelman JP, Maylie J, Sah P. Small-conductance Ca(2+)-activated K(+) channels: form and function. *Annu Rev Physiol* 2012;**74**:245–269.
2. Vergara C, Latorre R, Marrion NV, Adelman JP. Calcium-activated potassium channels. *Curr Opin Neurobiol* 1998;**8**:321–329.
3. Stocker M. Ca(2+)-activated K^+ channels: molecular determinants and function of the SK family. *Nat Rev Neurosci* 2004;**5**:758–770.
4. Xu Y, Tuteja D, Zhang Z, Xu D, Zhang Y, Rodriguez J *et al*. Molecular identification and functional roles of a Ca(2+)-activated K^+ channel in human and mouse hearts. *J Biol Chem* 2003;**278**:49085–49094.
5. Tuteja D, Xu D, Timofeyev V, Lu L, Sharma D, Zhang Z *et al*. Differential expression of small-conductance Ca^{2+}-activated K^+ channels SK1, SK2, and SK3 in mouse atrial and ventricular myocytes. *Am J Physiol Heart Circ Physiol* 2005;**289**:H2714–H2723.
6. Kohler M, Hirschberg B, Bond CT, Kinzie JM, Marrion NV, Maylie J *et al*. Small-conductance, calcium-activated potassium channels from mammalian brain. *Science* 1996;**273**:1709–1714.
7. Liegeois JF, Mercier F, Graulich A, Graulich-Lorge F, Scuvee-Moreau J, Seutin V. Modulation of small conductance calcium-activated potassium (SK) channels: a new challenge in medicinal chemistry. *Curr Med Chem* 2003;**10**:625–647.
8. Li N, Timofeyev V, Tuteja D, Xu D, Lu L, Zhang Q *et al*. Ablation of a Ca^{2+}-activated K^+ channel (SK2 channel) results in action potential prolongation in atrial myocytes and atrial fibrillation. *J Physiol* 2009;**587**:1087–1100.
9. Zhang Q, Timofeyev V, Lu L, Li N, Singapuri A, Long MK *et al*. Functional roles of a Ca^{2+}-activated K^+ channel in atrioventricular nodes. *Circ Res* 2008;**102**:465–471.
10. Monaghan AS, Benton DC, Bahia PK, Hosseini R, Shah YA, Haylett DG *et al*. The SK3 subunit of small conductance Ca^{2+}-activated K^+ channels interacts with both SK1 and SK2 subunits in a heterologous expression system. *J Biol Chem* 2004;**279**:1003–1009.
11. Ellinor PT, Lunetta KL, Glazer NL, Pfeufer A, Alonso A, Chung MK *et al*. Common variants in KCNN3 are associated with lone atrial fibrillation. *Nat Genet* 2010;**42**:240–244.
12. Ozgen N, Dun W, Sosunov EA, Anyukhovsky EP, Hirose M, Duffy HS *et al*. Early electrical remodeling in rabbit pulmonary vein results from trafficking of intracellular SK2 channels to membrane sites. *Cardiovasc Res* 2007;**75**:758–769.
13. Diness JG, Sorensen US, Nissen JD, Al-Shahib B, Jespersen T, Grunnet M *et al*. Inhibition of small-conductance Ca^{2+}-activated K^+ channels terminates and protects against atrial fibrillation. *Circ Arrhythm Electrophysiol* 2010;**3**:380–390.
14. Skibsbye L, Diness JG, Sorensen US, Hansen RS, Grunnet M. The duration of pacing-induced atrial fibrillation is reduced in vivo by inhibition of small conductance Ca(2+)-activated K(+) channels. *J Cardiovasc Pharmacol* 2011;**57**:672–681.
15. Hsueh CH, Chang PC, Hsieh YC, Reher T, Chen PS, Lin SF. Proarrhythmic effect of blocking the small conductance calcium activated potassium channel in isolated canine left atrium. *Heart Rhythm* 2013;**10**:891–898.
16. Chua SK, Chang PC, Maruyama M, Turker I, Shinohara T, Shen MJ *et al*. Small-conductance calcium-activated potassium channel and recurrent ventricular fibrillation in failing rabbit ventricles. *Circ Res* 2011;**108**:971–979.
17. Gui L, Bao Z, Jia Y, Qin X, Cheng ZJ, Zhu J *et al*. Ventricular tachyarrhythmias in rats with acute myocardial infarction involves activation of small-conductance Ca^{2+}-activated K^+ channels. *Am J Physiol Heart Circ Physiol* 2013;**304**:H118–H130.
18. Nattel S. New ideas about atrial fibrillation 50 years on. *Nature* 2002;**415**:219–226.
19. Bond CT, Sprengel R, Bissonnette JM, Kaufmann WA, Pribnow D, Neelands T *et al*. Respiration and parturition affected by conditional overexpression of the Ca^{2+}-activated K^+ channel subunit, SK3. *Science* 2000;**289**:1942–1946.
20. Glukhov AV, Fedorov VV, Anderson ME, Mohler PJ, Efimov IR. Functional anatomy of the murine sinus node: high-resolution optical mapping of ankyrin-B heterozygous mice. *Am J Physiol Heart Circ Physiol* 2010;**299**:H482–H491.
21. Glukhov AV, Flagg TP, Fedorov VV, Efimov IR, Nichols CG. Differential K(ATP) channel pharmacology in intact mouse heart. *J Mol Cell Cardiol* 2010;**48**:152–160.

22. Berul CI, Aronovitz MJ, Wang PJ, Mendelsohn ME. In vivo cardiac electrophysiology studies in the mouse. *Circulation* 1996;**94**:2641–2648.
23. Spani D, Arras M, Konig B, Rulicke T. Higher heart rate of laboratory mice housed individually vs in pairs. *Lab Anim* 2003;**37**:54–62.
24. Xing S, Tsaih SW, Yuan R, Svenson KL, Jorgenson LM, So M *et al*. Genetic influence on electrocardiogram time intervals and heart rate in aging mice. *Am J Physiol Heart Circ Physiol* 2009;**296**:H1907–H1913.
25. Lindsey ML, Escobar GP, Mukherjee R, Goshorn DK, Sheats NJ, Bruce JA *et al*. Matrix metalloproteinase-7 affects connexin-43 levels, electrical conduction, and survival after myocardial infarction. *Circulation* 2006;**113**:2919–2928.
26. Antzelevitch C. Heterogeneity and cardiac arrhythmias: an overview. *Heart Rhythm* 2007;**4**:964–972.
27. Chang PC, Hsieh YC, Hsueh CH, Weiss JN, Lin SF, Chen PS. Apamin induces early afterdepolarizations and torsades de Pointes ventricular arrhythmia from failing rabbit ventricles exhibiting secondary rises in intracellular calcium. *Heart Rhythm* 2013;**10**:1516–1524.
28. Qi XY, Diness JG, Brundel B, Zhou XB, Naud P, Wu CT *et al*. Role of small conductance calcium-activated potassium channels in atrial electrophysiology and fibrillation in the dog. *Circulation* 2013; [Epub ahead of print].
29. Oliveira MS, Skinner F, Arshadmansab MF, Garcia I, Mello CF, Knaus HG *et al*. Altered expression and function of small-conductance (SK) Ca(2+)-activated K^+ channels in pilocarpine-treated epileptic rats. *Brain Res* 2010;**1348**:187–199.
30. Kalume F, Westenbroek RE, Cheah CS, Yu FH, Oakley JC, Scheuer T *et al*. Sudden unexpected death in a mouse model of Dravet syndrome. *J Clin Invest* 2013;**123**:1798–1808.
31. Campen MJ, Tagaito Y, Li J, Balbir A, Tankersley CG, Smith P *et al*. Phenotypic variation in cardiovascular responses to acute hypoxic and hypercapnic exposure in mice. *Physiol Genomics* 2004;**20**:15–20.